Journal of South American Earth Sciences 28 (2009) 374–382

Contents lists available at ScienceDirect

Journal of South American Earth Sciences

journal homepage: www.elsevier.com/locate/jsames

Basic magmatism in northeastern Puna, Argentina: Chemical composition and tectonic setting in the Ordovician back-arc

Beatriz Coira [a,*], Alicia Kirschbaum [b,c], Fernando Hongn [b,c], Belén Pérez [a], Nilda Menegatti [b]

[a] CONICET, Instituto de Geología y Minería, Universidad Nacional de Jujuy, CC 258, 4600 San Salvador de Jujuy, Argentina
[b] Universidad Nacional De Salta, Facultad de Ciencias Naturales, Av. Bolivia 5150, 4400 Salta, Argentina
[c] CONICET–IBIGEO, Museo De Ciencias Naturales, Facultad de Ciencias Naturales, UNSa, Mendoza 2, 4400 Salta, Argentina

ARTICLE INFO

Keywords:
Northeastern Puna
Ordovician
Back-arc magmatism
Extensional-contractional episodes
Argentina

ABSTRACT

Two main groups of basic rocks, representative of the bimodal Ordovician magmatism of the northeastern Puna (22–24°S, 66°30'–65°40'W) were revisited on the basis of new geological, petrographic and geochemical data. One of them shows geochemical characteristics intermediate between those of MORB and arc-type basalts common in back-arc basins. The other group is represented by low and high Ti basalts and gabbros with an OIB-type signature. Basalts of the first group (Tremadocian–early Arenigian) along with minor dacites are found within a sedimentary–volcanic sequence that hosts the Cobres and the Tanque granitic plutons (475–480 Ma). This group of basic rocks is also coeval with Cobres Granite, whereas magmas with OIB-type signature were contemporary with the emplacement of Tanque Granite. During the early to middle Arenigian, dacites and minor amounts of basalts with OIB-type signatures erupted in the Escaya–Huancar ranges and were intruded as dikes in Cobres and Tanque ranges.

Two main stages are recorded in the tectono-magmatic evolution of the region. The first stage was dominated by extension (Tremadocian–early Arenigian), and the second (until the late Arenigian) during which extensional and contractional conditions occurred diachronously along the basin. The geochemical characteristics of the basic magmas are attributed to a combination of factors such as variably depleted mantle sources, continental crustal contamination and addition of subduction components, as well as variations in the degree of melting in the sources.

These factors probably were controlled by episodical changes both in time and space in the extensional conditions. These characteristics altogether indicate a back-arc setting for the northeastern Puna during Early and Middle Ordovician, in which contractional episodes took place.

1. Introduction

Petrologic investigations carried out to contribute to geodynamic models for the Argentine Puna during the early Paleozoic (Koukharsky et al., 1989; Coira and Koukharsky, 1991; Bahlburg, 1990; Pérez and Coira, 1998; Coira et al., 1999; Lucassen et al., 1999; Bock et al., 2000; Lucassen et al., 2001; Zimmermann and Bahlburg, 2003; among others) have produced an important geochemical and isotopic database of igneous, metamorphic and sedimentary rock suites. This information has significatively contributed to enlarge our knowledge of the nature of the crust, and of its evolution at that in the early Paleozoic time. Basic igneous rocks, however, are poorly represented in this database. This work is focused on the petrology of the Ordovician basic rocks from the northeastern Puna, to evaluate the degree and type of mantle contribution to the continental crust, and to better constrain the tectonic setting of this segment of the proto-Andean western Gondwana margin during the lower Paleozoic.

Basic magmatism was long recognized in the Puna pre-Andean basement (Pérez and Coira, 1998; Coira et al., 1999; Coira and Koukharsky, 2002; Kirschbaum et al., 2005; among others). In the Cochinoca–Escaya range (Fig. 1), Coira et al. (1999) and Coira et al. (2004) described lava flows, sills and basic dykes that along with dacitic volcanic–subvolcanic units constitute the early to middle Arenigian Cochinoca–Escaya Magmatic–Sedimentary Complex. In the Tanque range, Pérez and Coira (1998) described basic and siliceous lava flows, sills and dykes in the Early Ordovician sedimentary sequence that hosts the syntectonic Tanque Granite. This granite shows mixing and mingling with gabbroic magmas.

In the southern Puna, Coira et al. (2002) recognized basic magmatic rocks represented by fine-grained gabbros, microgabbros and basalts with transitional characteristics between volcanic arc tholeiitic basalts and MORB-type, intercalated within an early Paleozoic turbiditic clastic sequence in the Quebrada Honda range.

* Corresponding author. Fax: +54 388 4232957.
E-mail addresses: bcoira@idgym.unju.edu.ar (B. Coira), alikir@unsa.edu.ar (A. Kirschbaum), hongn@unsa.edu.ar (F. Hongn), nilda@unsa.edu.ar (N. Menegatti).

0895-9811/$ - see front matter © 2009 Elsevier Ltd. All rights reserved.
doi:10.1016/j.jsames.2009.04.007

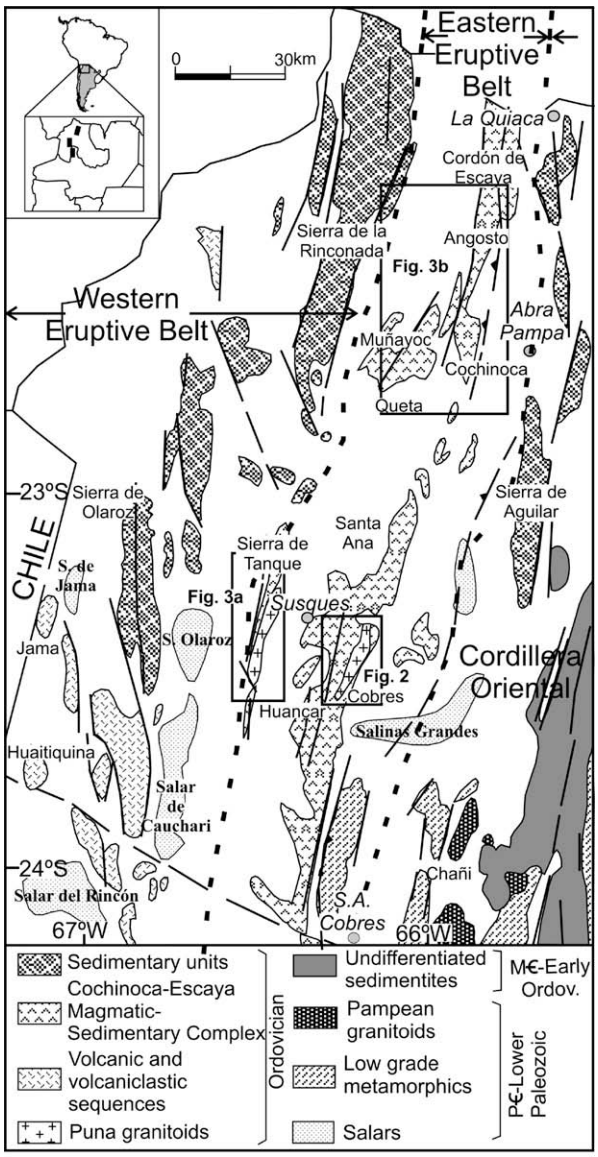

Fig. 1. Map showing the distribution of lower Paleozoic magmatic and sedimentary units in the Northern Puna. Frame localities are analyzed in the text and considered in detail in Figs. 2 and 3a and b.

Coira and Darren (2002) identified alkaline lamprophyres conformably intercalated within an early Arenigian clastic sequence in the Sierra range (Jujuy province). Gabbros and microgabbros were also found in the Cobres range (Kirschbaum et al., 2005).

Regional isotopic and geochemical studies on lower Paleozoic volcanic and sedimentary rocks from the Puna (Bahlburg, 1990; Bock et al., 2000; Lucassen et al., 2000 have been interpreted to indicate that input from juvenile magmatic sources was minor. These authors concluded that there was not any significant crustal growth during the early Paleozoic. Bock et al. (2000) restrict the input of juvenile material to a short time during the Arenigian.

Analysis of the tectono-magmatic evolution of northeastern Puna during the early Paleozoic, especially in the Ordovician, has shown that extensional, contractional and strike-slip regimes overlapped each other, leading to a complex kinematic evolution (Bahlburg, 1990; Hongn, 1994; Hongn and Mon, 1999). Because the studied basic rocks were recorded in different tectonics frameworks and at different times they are useful to unravel the Ordovician geodynamic evolution of the Puna.

Representative sequences of Ordovician basic igneous rocks from northeastern Puna were selected for petrography and geochemistry along cross-sections between 22° and 24°S (Fig. 1). The new data along with previous results allow us to better constrain the magma sources and evolution, and to adjust the geodynamic scenario for the Puna during the Ordovician.

2. Geological setting

An extensive Ordovician magmatism began in the Puna in the early Tremadocian, and it reached the climax in the middle Arenigian. The basic rocks occur in two submeridian magmatic belts known as the Western Eruptive Belt (Palma et al., 1986) and Eastern Eruptive Belt (Méndez et al., 1973). Ordovician magmatic rocks in the northern Eastern Puna Eruptive Belt (Fig. 1) occur in a bimodal volcanic and plutonic magmatic suite of Early Ordovician age. These syn-sedimentary volcanic and subvolcanic rocks (dacites and minor (5–10%) basalts and microgabbros) associated with clastic sequences are affected by green-schist facies metamorphism. In the Cochinoca–Escaya region these units constitute the Cochinoca–Escaya Magmatic–Sedimentary Complex (Coira et al., 1999; Coira et al., 2004) that contains a graptolite fauna of late Tremadocian to early-middle Arenigian age (Bahlburg 1990; Martínez et al., 1999; Benedetto et al., 2002). This complex records Ordovician folding, which shows a well-defined lithological control; so tight folds are common in pelite-dominated successions whereas open folds develop in volcanic intercalations. Folds strike NE–SW in the Queta and Quichagua ranges, and their axial surfaces dip towards the NW. In the Cochinoca–Escaya range, the structures strike approximately north–south. Axial lines plunge smoothly. Relations between fold axes and stretching lineation indicate variations in the strike-slip component (Hongn, 1994).

In the Huancar, Sey and Taique regions (Fig. 1), the volcano-sedimentary sequence represented by dacitic and minor (<2%) basic lavas, domes and sills syn-depositional with thick turbidites were attributed to the Chiquero Formation (Schwab, 1973; emend Coira et al., 2005). They were assigned to late Tremadocian according to their fossil content (Benedetto et al., 2002).

Intrusive rocks crop out in Cobres and Tanque ranges (Figs. 2 and 3a). The Cobres Plutonic Complex consists of two main plutons: granodiorite (476 ± 1 Ma U/Pb age on monazite, Lork and Bahlburg, 1993) and monzogranite (478.4 ± 3.5 Ma zircon U/Pb age; Haschke et al., 2005), a leucogranite stock, acid dikes and small bodies of microgabbros and gabbros (2–3%). The country rock corresponds to sandstones and pelites with intercalations of basic volcanic rocks. Thermal metamorphism transformed the country rock to spotted phyllite-schist and to schist and gneiss (Fig. 2). High-T ductile deformation zones concentrate around the contact between granodiorite and host rock recording higher metamorphic grade (Hongn et al., 2006). The shallow–plunging stretching lineation (Fig. 2) and some steep-plunging fold axes point to strike-slip components in the kinematics of the Ordovician deformation (Bahlburg, 1990; Hongn and Mon 1999).

The Tanque Plutonic Complex (Fig. 3a) consists mainly of granular syntectonic monzogranite with minor porphyritic fabric, which shows mixing and mingling relations with gabbro rocks (10%). Granite as well as gabbro shows a heterogeneously developed foliation. As described in Cobres, the country rock shows thermal metamorphism spatially related to the intrusion. However, as observed in other areas with Ordovician intrusions, metamorphism seems to be related to a rather regional thermal anomaly extended along the southeastern border of the Puna and northern Pampen ranges (e.g. Lucassen and Becchio, 2003). Nevertheless, the sub-vertical foliation and lineation observed in high temperature deformation belts suggest dominantly contractional

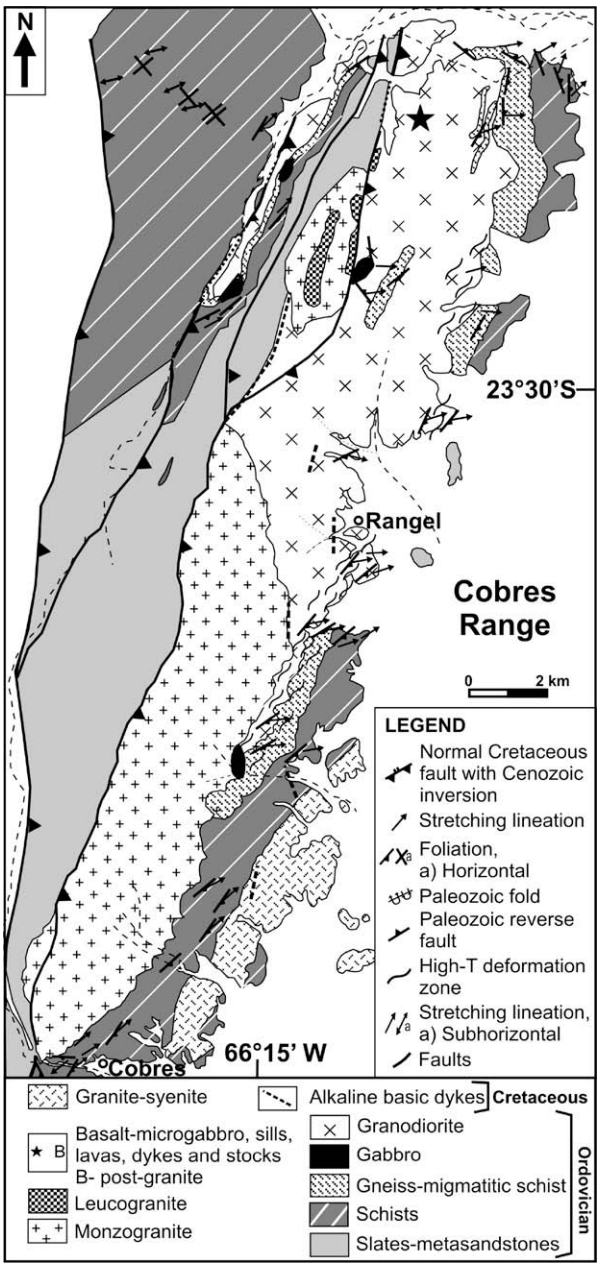

Fig. 2. Geological map of Cobres range with details of the magmatic Ordovician units discussed in text. Map modified from Hongn et al. (2006).

kinematics, with no strike-slip component being detected as in Cobres. The Tanque pluton yielded a monazite U/Pb age of 479 ± 1.7 Ma (Coira, unpublished). Similar lithologies and ages, as well as high-T deformation in plutonic and host rocks and their similar fabric orientation, strongly suggest that Cobres and Tanque plutons are related to a syntectonic magmatism that took place between 480 and 475 Ma.

The Western Eruptive Belt includes the Tremadocian–Arenigian magmatism recorded in western Puna and north of Chile. The first cycle in this belt started with basaltic–andesitic lavas, some of them showing pillow structures, intercalated within a shallow marine sedimentary sequence (Niemeyer, 1989). These lavas show a composite geochemical signature of MORB and tholeiitic arc basalts, characteristic of a supra-subduction setting (Breitkreuz et al., 1989; Coira et al., 2002). They were followed by dacitic–rhyolitic pyroclastic sequences ending under subaerial conditions (Koukharsky et al., 1996). This first cycle ended with the intrusion of plutons during upper Tremadocian–early Arenigian (Blasco et al., 1996; Koukharsky et al., 2002; Kleine et al., 2004). The second cycle during Arenigian is represented by basaltic–andesites to andesites with arc to back-arc geochemical signature (Coira et al., 1999) developed in a shallow marine environment. During this time, a back-arc basin evolved in north-eastern Puna, along with the bimodal magmatism recorded in the Eastern Eruptive Belt.

3. Basic magmatism in Cobres range

Ordovician basic rocks in the Cobres range show variable relationships with the siliceous plutonic rocks of the Cobres Complex (Fig. 2). They are gabbro and microgabbro bodies that range between a few centimeters to tens of meters in width, dark grey to black in color, sometimes greenish, due to alteration processes. Field relationships among basic rocks and granitic plutons permit us to distinguish them into three groups:

3.1. Pre-granite basic rocks

These are greenish lensoidal bodies, concordant with and folded along with bedding of the metasedimentary country rock. Lensoidal shape results from boudinage because of competent behavior. These bodies correspond to volcanic intercalations whose primary features were obliterated by regional metamorphism (deformation and recrystallization along with weak cataclasis). Tremolite–actinolite, the main component is observed surrounding plagioclase, opaque minerals, titanite and epidote. Biotite in small crystals and in strips indicates a secondary foliation.

3.2. Syn-granite basic rocks

These correspond to gabbros that crop out as partially dismembered and brecciated bodies with tabular to lensoidal shapes and 4–6 m in thickness. These gabbroic rocks are always parallel and concordant to the contact between the granodiorite and the metamorphic country rock or to the contact between different granodioritic sheets (Fig. 2). Gabbros in contact with the granodiorite show a narrow external zone of finer grain. This feature along with well-defined magmatic orientation of K-feldspar crystals in granodiorite indicates that gabbros and granodiorite are contemporaneous. Within this group of basic rocks there are porphyritic and granular ones. The former exhibit phenocrysts of plagioclase (1.6–2.8 mm) intensely replaced by sericite and epidote and of pyroxene entirely converted to calcite and argillic minerals, in a coarse grained groundmass (0.20–0.25 mm) composed by hornblende and plagioclase with titanite and opaque minerals. Granular gabbros are equigranular, fine grained (0.5–0.6 mm), melanocratic, composed by hornblende and andesine with opaque minerals, apatite, zircon and as secondary minerals, chlorite, epidote and sericite.

3.3. Post-granite basic rocks

These correspond to microgabbro bodies that intrude discordantly into the country rock and the granodiorite. The microgabbros are fine grained (0.6–0.8 mm) to scarcely porphyritic, composed by plagioclase, hornblende, relictic clinopyroxene, titano-ilmenite, apatite, zircon and as secondary minerals chlorite, sericite and argillic minerals. Although, this group of basic rocks shows similar field relationships to alkaline Cretaceous dikes (basalts, trachybasalts and tephrites), which are not considered here. Those Cretaceous rocks can be distinguished by their alkaline mineralogy, such as ferro-edenite, and their geochemical alkaline signature (Kirschbaum et al 2006).

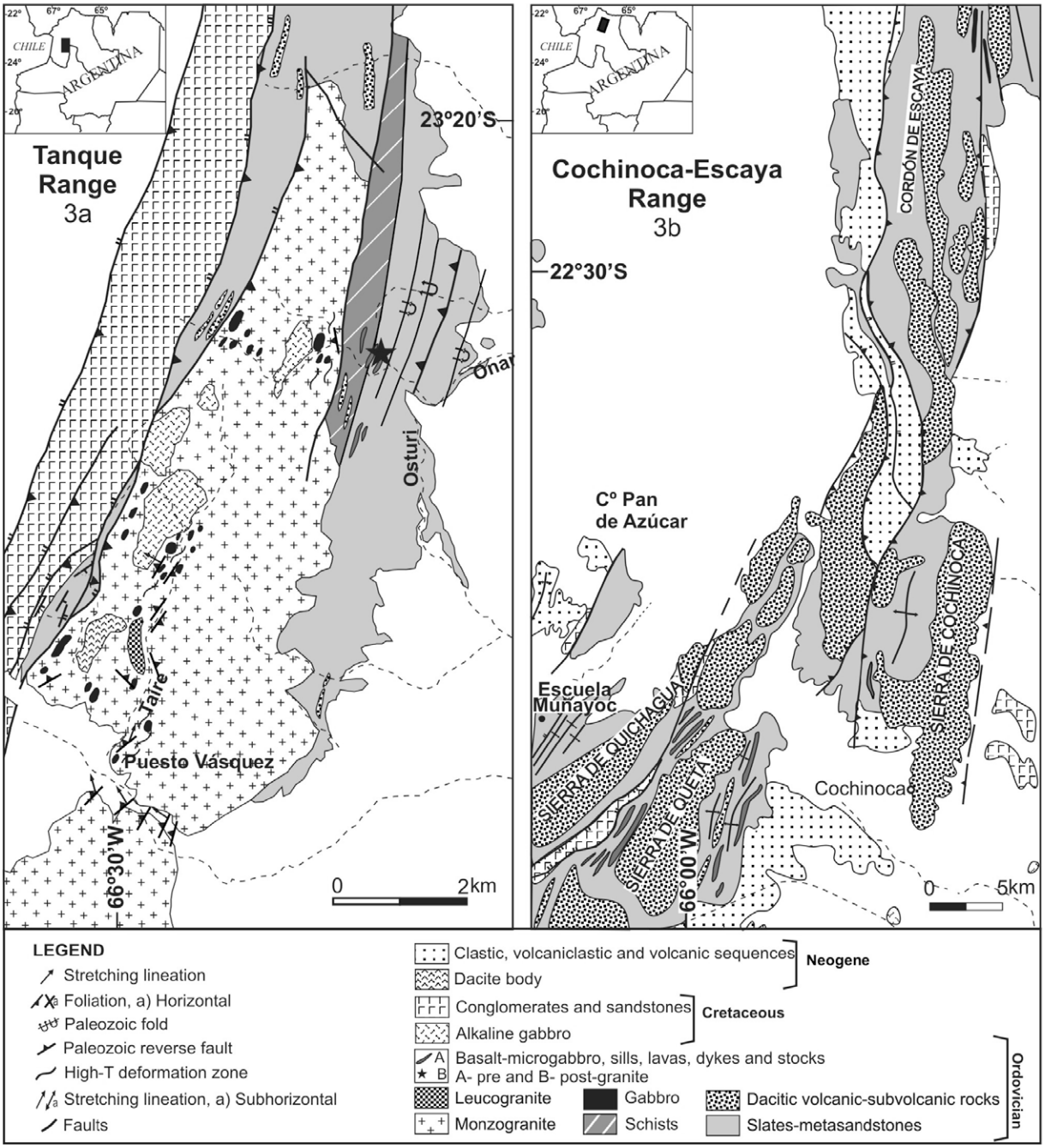

Fig. 3. (a) Geological map of Tanque and (b) of Escaya–Cochinoca ranges showing the magmatic units analyzed.

4. Basic magmatism in the Tanque range

Basic sills and dikes (basalts and microgabbros) occur in the Early Ordovician sedimentary sequence that hosts the syntectonic Tanque Granite (Fig. 3a). They form generally concordant bodies with the sedimentary rocks that range from 2 to 6 m in thickness. Folding of Ordovician age affects both the basic and sedimentary rocks. The generally altered spilitic basalts have vesicular, aphanitic to scarcely porphyritic textures. They are made up of fine chloritized or albitized plagioclase laths in a clinochlore and calcitic mesostasis groundmass that are associated with partially chloritized amphibole that shows a sub-ophitic relation with plagioclase and opaque minerals. The vesicles, 0.5–3 mm in diameter, are filled with chlorite and carbonate aggregates. The fine granular microgabbros generally have ophitic textures and are mainly composed of plagioclase and clinopyroxene associated with tremolite, chlorite, titanite, apatite and opaque minerals. As in the Cobres area, these basic rocks are deformed along with the metasedimentary host rocks. They are boudinaged to variable degrees, depending on the thickness of the basic rock. The gabbros of the plutonic complex that constitutes the core of the Tanque range form small bodies (<20 m lengthwise). They are usually foliated and elongated in concordance with the foliation of the granite (Fig. 3a) and show evidence for mingling and mixing relations with the granite. Both the granite and the gabbro rocks exhibit high temperature deformation fabrics, documented by "granitic striped gneisses" in which K-feldspar shows dynamic recrystallization and quartz develops chessboard fabric. The gabbros essentially consist of plagioclase and titanaugite replaced by hornblende along with abundant titanite and acicular apatite. They show variable foliation that is marked

by segregations of plagioclase-rich stripes and subparallel bands with plagioclase, hornblende and opaque minerals.

Post-granite basic dikes (1–2 m thick) discordantly intrude the sedimentary–magmatic sequence and the granite. They are represented by microgabbros to microdiorites of fine grain (1–4 mm) to scarcely porphyritic, mainly composed of plagioclase (andesine-labradorite) partially altered to sericite and epidote and hornblende with apatite and opaque minerals as accessories. As in the Cobres area, mineralogy permits us to distinguish these Paleozoic basic rocks from those of Cretaceous age showing similar discordant field relationships.

5. Basic magmatism in Cochinoca–Escaya range

Basic rocks in the Cochinoca–Escaya range are represented by lava flows, sills and laccoliths up to 30 m thick, syn-depositional with thick psamitic–pelitic sequences (Fig. 3b), altogether deformed. In some cases they present peperites at their bases and/or roofs, indicating their interaction with water-saturated hosting sedimentary rocks. Within them, moderately to intensely altered basalts (spilites) and microgabbros are recognized.

The spilitic basalts are usually arranged as sills and lavas, locally with pillow structures (Coira and Koukharsky, 1991). They are constituted by non-oriented plagioclase laths 0.3–0.5 mm in diameter, albitized and replaced by sericite–chlorite and carbonates, among which chlorite aggregates, abundant titanite, apatite, and skeletal opaque minerals turning into leucoxene are distributed. In a few cases it is possible to recognize pyroxene relictic crystals. A remarkable NNE to N-striking foliation that overprints at variable degrees the volcanic textures develops in the thinnest (3–5 ms) and most altered basalts.

The microgabbros constitute sills and laccoliths, and in a few cases dikes that discordantly cut the clastic sequence. They are distinguished from the basalts by their greater grain size and lower

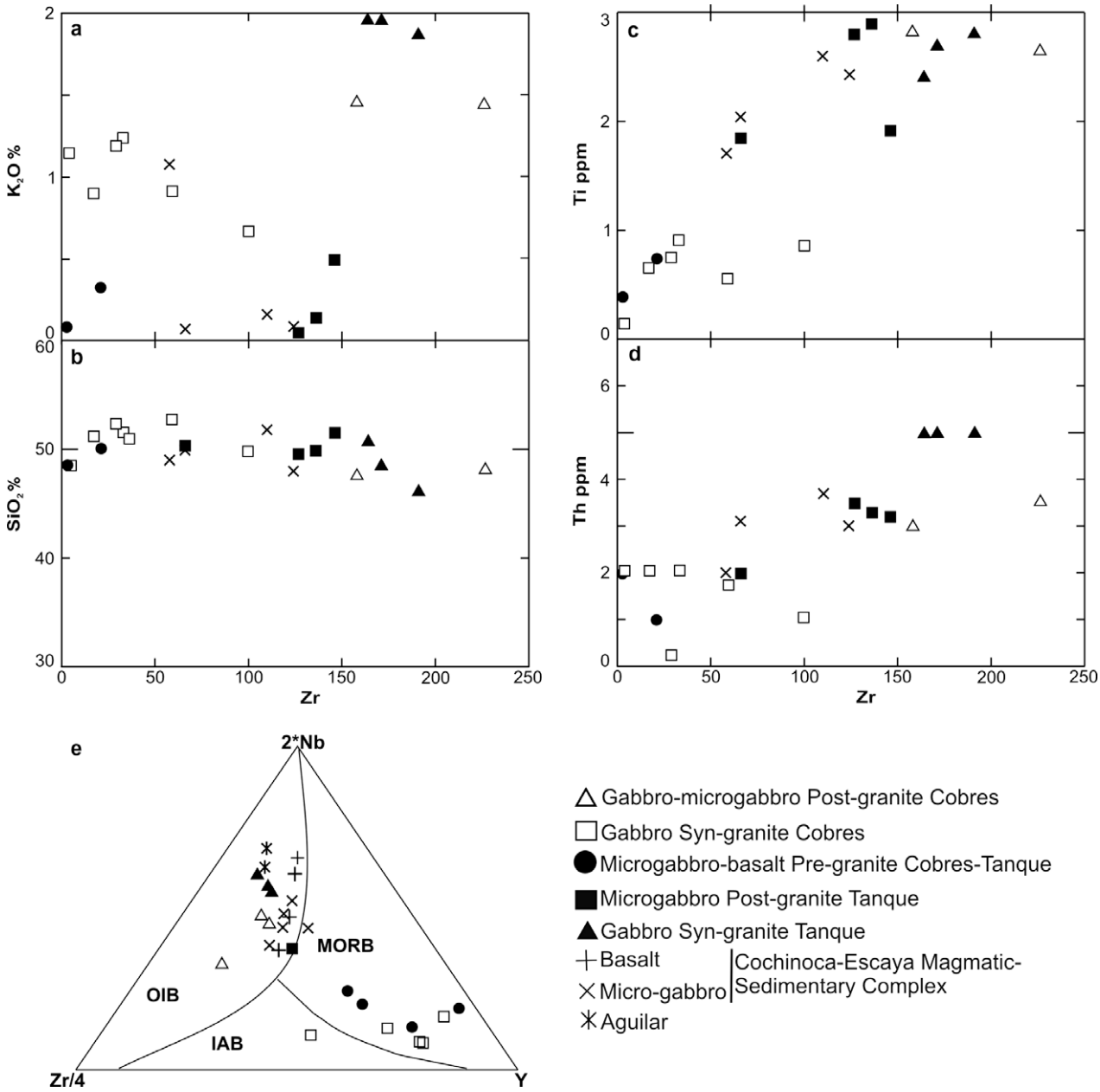

Fig. 4. (a–d) Plots of K_2O, SiO_2 (in wt%), Ti and Th (in ppm) vs. Zr. Note the positive correlation between Zr–Ti and Zr–Th, see text for discussion. (4e) Geotectonic discrimination diagram from Vermeesch (2006).

alteration stage. They are constituted by clinopyroxene (augite–titanaugite) in crystals 5–8 mm in diameter and plagioclase in ophitic relation distributed inside a chloritic matrix, accompanied by abundant titanite, apatite and opaque minerals. Along with chlorite, they usually show epidote and calcite aggregates that pseudomorphically replace the plagioclase and clinopyroxene crystals or irregularly and/or in the shape of veins replace the whole of the sample.

6. Geochemistry

In the study area, Ordovician basic rocks have been modified by superimposed hydrothermal alteration and/or metamorphism. The HFSE elements, including Hf, Ti, Nb, Ta, Zr, Sc, Y are considered to be immobile during these processes, as has been confirmed by numerous studies of fresh, altered and metamorphosed basic rocks (Cann, 1970; Pearce and Cann, 1973;Winchester and Floyd, 1977; Pearce and Norry, 1979; Pearce, 1996). The degree of geochemical modification of the analyzed rocks may be illustrated in Fig. 4, where K_2O, SiO_2, Ti and Th are plotted against Zr. Ti and Th show strong positive correlation while the mobile elements Si and K have a great dispersion (Fig. 4a–d). It can thus be inferred that Ti and Th were almost unaffected by weathering and metamorphism.

The basic rocks that are pre- and syn-granite in age in the Cobres range and pre-granite in the Tanque range (48–52% SiO_2) have low TiO_2 (0.2–0.9%) and P_2O_5 (0.01–0.15%) contents, Nb/Y ratios of less than 0.4, and low Zr and Nb contents (Table 1). On the Zr/4–2Nb–Y discrimination diagram, they plot in the MORB and IAB fields (Fig. 4e). On an extended trace element diagram normalized to MORB (Fig. 5b), these basic rocks (Cobres pre- and syn-granite and Tanque pre-granite) have E-MORB-like patterns showing Th and LREE enrichment (La/Th = 2.2–6) and at the same time Nb depletion relative to Th and La (e.g. La/Nb = 1.2–2.7), which is distinctive of arc basalts. This geochemical signature is commonly observed in back-arc basin basalts (BABB) reflecting the contribution of LIL-enriched hydrous fluids related to the subduction component and the HFSE depletion relative to the mantle (Hawkins, 1970; Fryer et al., 1990; Saunders and Tarney, 1984; Hawkins, 1995).

In contrast with the previous rocks (group A), the Cobres and Tanque post-granite basic rocks together with the Tanque syn-granite gabbros (46–52% SiO_2) show an OIB-like signature

Table 1
Analysis of basic selected rocks of the northeastern Puna. Major elements (wt%), trace elements (ppm). Analytical methods: geochemical analyses of major elements and some trace elements (Rb, Ba, Sr, Y, Zr, Hf, Nb, Th, U, Co, Cr, Ni, and V) were carried out in the FRX laboratory of the Instituto de Geología y Minería (UNJu) with a Rigaku FX2000 spectrometer, with Rh tube, operating at 50 kV and 45 mA, under USGS and Japan Geological Survey standards. Rare earths analysis of REE, Sc, Th, U, Hf, Cs, and Ta were determined by INAA at LAAN, Centro Atómico Bariloche, using the absolute parametric method. Irradiations were performed in the RA-6 reactor, the gamma spectra were measured with an HPGe detector of 12.3% relative efficiency at 1.33 MeV and data collection was performed with a multi-channel ND76 analyzer bearing 4096 channels, applying the GAMANAL routine of the GANAAS (IAEA/CMS/3, 1991) package.

Lithology	Cobres range										Tanque range			Queta range	
	Gabbro–microgabbro										Basalt	Gabbro		Basalt	Microgabbro
	△			□					●		●	▲		+	×
Sample	CO3–5a	CO3–5b	CO3–8	CO1–15	CO1–9	CO3–14a	CO3–23a	CO1–11	CO3–25a	CO3–25b	BT34	JE–31	Va–6	BC32A	BC35
SiO_2	47.15	47.54	47.98	51.36	51.04	49.61	52.13	48.31	48.57	50.11	49.29	50.81	48.6	48.98	49.86
TiO_2	2.43	2.81	2.50	0.90	0.64	0.84	0.73	0.13	0.39	0.74	1.18	2.41	2.70	1.70	2.89
Al_2O_3	16.92	16.02	16.54	15.23	15.00	14.02	16.43	18.08	12.68	14.03	16.09	13.97	14.08	16.75	16.79
Fe_2O_3	10.54	11.01	10.24	9.69	9.68	10.18	8.18	6.58	6.89	10.04	10.35	9.15	9.65	9.83	12.53
MnO	0.13	0.15	0.16	0.08	0.18	0.17	0.17	0.11	0.18	0.18	0.19	0.16	0.17	0.16	0.22
MgO	6.76	6.90	7.30	7.82	8.12	8.01	7.15	10.49	18.47	9.48	9.28	8.09	7.15	6.69	5.82
CaO	9.08	8.76	9.88	9.57	11.49	10.49	10.89	12.31	9.94	11.24	9.68	8.22	10.82	12.09	6.97
Na_2O	2.73	3.05	2.62	2.61	1.89	2.01	2.67	0.82	0.27	1.68	1.88	2.92	3.24	1.20	4.45
K_2O	1.95	1.45	1.40	1.23	0.89	0.65	1.18	1.13	0.08	0.32	0.56	1.96	1.96	1.07	0.13
P_2O_5	0.42	0.39	0.37	0.06	0.05	0.07	0.07	0.01	0.04	0.06	0.15	0.44	0.49	0.22	0.35
LOI	1.25	1.85	1.29	0.69	0.82	1.14	0.88	2.26	1.05	2.56	2.65	1.17	0.60	1.40	2.94
Total	99.35	99.93	100.26	99.24	99.79	97.19	100.48	100.23	98.56	100.44	98.65	99.30	99.46	100.19	100.01
V	280	–	277	–	–	302	244	–	–	–	3	240	308	210	343
Cr	11	84	108	242	317	183	164	245	366	354	5	443	227	1260	27
Co	48	49	47	41	44	56	51	46	69	55	76	42	37	30	57
Ni	73	55	78	80	61	75	46	171	559	149	115	120	66	125	4
Rb	161	55	104	80	56	41	133	65	9	21	31	74	84	58	11
Sr	451	299	425	116	90	200	208	118	4	70	163	348	428	430	290
Y	23	25	24	34	18	24	20	9	16	21	23	24	23	14	27
Zr	278	158	255	33	17	100	29	4	3	21	43	164	171	58	136
Cs	16	–	9	–	–	2	4	–	–	–	3	18	16	2	–
Ba	309	624	184	183	105	199	45	49	39	86	96	516	565	485	238
Nb	26	29	23	2	1	2	4	1	2	2	6	41	46	22	24
Hf	5	4	5	2	1	2	1	1	2	2	2	6	6	3	5
Ta	2	–	1.8	–	–	<1	<1	–	–	–	<1	3.7	3.8	2	–
Th	3	3	3	2	2	1	<1	2	2	1	<1	6	7	2	3
U	1	1	1	1	1	1	1	1	1	1	1	3	3	1	1
Sc	19	–	30	–	–	41	39	–	–	–	3	25	32	42	–
La	29	–	26	–	–	5	3	–	–	–	5	38	46	15	–
Ce	62	–	55	–	–	12	9	–	–	–	13	76	93	33	–
Nd	36	–	34	–	–	13	6	–	–	–	Nd	37	41	15	–
Sm	7	–	7	–	–	2	2	–	–	–	2	7	9	4	–
Eu	2	–	2	–	–	1	1	–	–	–	1	2	3	1	–
Tb	1	–	1	–	–	1	1	–	–	–	1	1	1	1	–
Dy	6	–	6	–	–	5	4	–	–	–	4	6	7	–	–
Yb	2	–	2	–	–	3	2	–	–	–	3	2	2	2	–
Lu	<1	–	<1	–	–	<1	<1	–	–	–	<1	<1	<1	<1	–

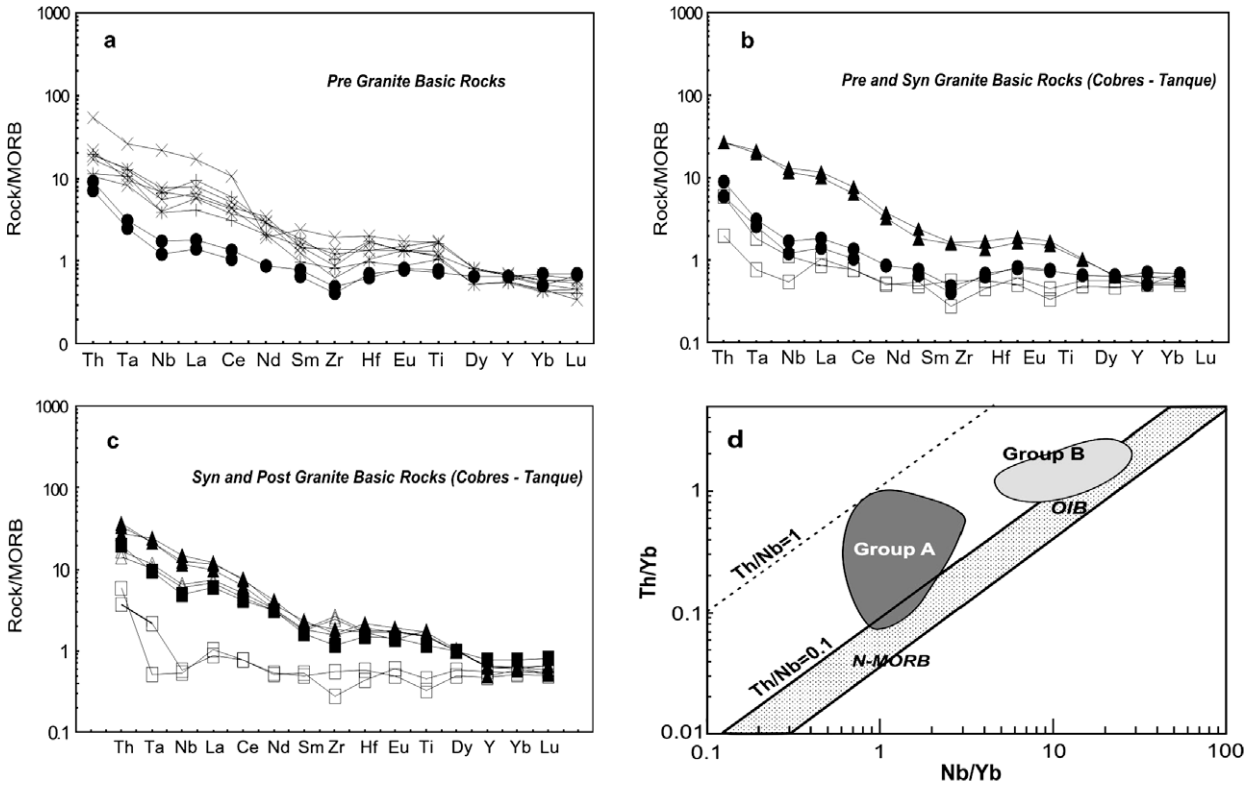

Fig. 5. (a–c) Extended trace element spider-diagrams of pre-, syn- and post-granite basic rocks from northeastern Puna. N-MORB normalization values after Hofmann (1988). Data from Table 1. Symbols as Fig. 4d) Th/Yb–Nb/Yb diagram. The alkaline group of basic rocks (A) plot apart from the subalkaline group (B) within a mantle array (shaded field) between N MORB and OIB basalts.

(Fig. 5c). These rocks (group B) are enriched in TiO_2 (1.8–2.8%), P_2O_5 (0.35–0.65%), Nb (Table 1) and have Nb/Yb = 8–11 and La/Ta = 10–13; they also exhibit a notable enrichment in Th, Ta, Nb, as well as steep REE patterns (La/Yb = 11–21). In the extended trace element diagrams in Fig. 5b, this group is clearly differentiated from group A, characterized by MORB affinities.

The Cochinoca–Escaya basic group of rocks (46–52% SiO_2 content) are characterized by high Nb/Yb (8–30) and Th/Yb (1–2) and low La/Ta (10–15) ratios indicating also an OIB signature. As discussed by Coira et al. (1999), this can be divided into low-Ti and high-Ti types. The low-Ti type is light REE enriched, has TiO_2 contents of 1.1–2.1%, low K_2O (<0.6%) and La/Th ratios from 6.5 to 11. The high-Ti type has lower SiO_2 (42–51%), higher TiO_2 (>2.1%) and K_2O (up to 2.2%) concentrations. They have steeper REE patterns with similar low La/Ta ratios = 10–13 (Fig. 5a).

In the Th/Yb–Nb/Yb diagram (Fig. 5d) samples of group A plot between the N-MORB field on the mantle array and the Th/Nb = 1 line, whereas samples of group B fall near the OIB field, but at higher Nb/Yb ratios. In both cases, but more strongly in group A, the samples plot above the mantle array. Their higher Th/Nb ratios are indicative of a continental crust addition and/or fluid-dominated subduction component added to the mantle source (Pearce et al., 1984).

Nd isotopic data for spilitic basalts and microgabbros from Cochinoca–Escaya ranges have initial εNd values at 475 Ma that range from 4 to 7.6 (Bierlein et al., 2006) and the Cobres post-granite basic rocks have a value of 4 (Kirschbaum et al., unpublished data), indicating a juvenile input at that time in those regions. Conversely, the samples from group A (Cobres syn-granite gabbro and Tanque pre-granite basalt) have initial εNd values at 475 Ma from 4 to 0.4. Taking into account the crustal εNd initial −5 to −10 and TDM model ages between 1.6 and 1.8 Ga determined for the basement rocks in the region (Bock et al., 2000; Lucassen et al., 2000), the less radiogenic Nd isotope values of these samples could be attributed to a larger crustal contamination with early Proterozoic felsic crust, a characteristic that was previously pointed out in Fig. 5d.

7. Discussion and conclusions

The basic rocks with MORB-arc (group A) and OIB signature (group B), together with the voluminous mesosilicic volcanic rocks with crustal affinities, record a bimodal magmatic episode that occurred during the Tremadocian–Arenigian in the studied region. The oldest basic magmatic rocks that preceded the emplacement of the late Tremadocian Cobres and Tanque granitoids show a signature that is intermediate between MORB and arc basalts. These are features typical of back-arc basin basalts (BABB, Pearce et al., 1984). In the Tanque and Huancar ranges those basic rocks coexist with dacitic sills and laccoliths that have crustal signatures and are syn-depositional with sedimentary sequences of late Tremadocian–Arenigian age (Coira et al., 1999). The basic rocks associated with the granitoids show two affinities: MORB-arc in the Cobres range and OIB in the Tanque region. The thermal peak represented by this plutonic event at the Tremadocian–Arenigian boundary was contemporary with the first emplacement of OIB-like basic rocks in the region, as in the case of the Tanque granitoid. The last post-Cobres and Tanque granite basic rocks and the volcanic–subvolcanic basic rocks in the Escaya–Cochinoca ranges all show OIB signatures. The Cochinoca–Escaya basic alkaline rocks are also contemporaneous, as in Tanque and Huancar regions, with dacitic rocks that have crustal affinities (Coira et al., 1999) and are associated with early-middle Arenigian clastic sequences. The temporal variation

between the volcano-sedimentary records in the Tanque and Huancar ranges in the south, and in the Cochinoca–Escaya region in the north, denotes diachronism in those events along the northeastern Puna, accompanied by compositional differences in the basic rocks.

The spider diagrams (Fig. 5a, b and c), Th/Yb vs. Nb/Yb plot (Fig. 5d) and isotopic data presented support a MORB signature for basic rocks of group A and OIB affiliation for group B, as well as a variable degree of contamination with early Proterozoic felsic crust, and a possible contribution of fluid-dominated subduction component added to the mantle sources.

On other hand, variations of the chemistry of the younger high and low Ti OIB rocks can be interpreted as indicating a different percentage of melting of chemically similar spinel and garnet-bearing peridotite sources.

Coira et al. (1999) suggested that the Ordovician magmatism in the northern Puna took place in a transpressive setting in which the strike-slip component gave way to dilation zones in which magmas ascended and emplaced, whereas Kirschbaum et al. (2006) suggested that the bimodality could result from an extensional tectonic regime in which short periods of contractional deformation can occur following the model of extensional accretionary orogens (Collins, 2002). The integration of these two proposals with our new data allows a tectonic model that explains our observations.

The alternate and diachronic distribution of magmatic events with different crustal and mantle affinities suggests that the evolution of the Ordovician basins included periods and areas of extensional and contractional deformation.

A model that integrates published information (Bahlburg and Hervé, 1997; Coira et al., 1999; Zimmermann and Bahlburg, 2003) with the magmatic data summarized here fits with a magmatic arc to the west of a back-arc in Tremadocian–middle Arenigian times. The tectonic setting was not simple, as the back-arc was active over a long time (~15 Ma) and records contractional and strike-slip events occurring at distinct times and places in an overall extensional framework. Contractional deformation with variable components of strike-slip took place contemporaneously with the intrusion of upper Tremadocian–lower Arenigian bimodal plutonism in the Cobres and Tanque ranges (Kirschbaum et al., 2006; Hongn et al., 2006). Bimodal volcanism occurred in the middle Arenigian in the Cochinoca–Escaya ranges, indicating that in this region extension continued until the middle Arenigian.

During the Arenigian a transition from extensional to contractional conditions began (Bahlburg, 1990). By the Llanvirnian, a well-defined contractional environment was in place. This transition involved some localized shortening in a generally extensional framework due to kinematic variations of the subduction under the western arc. Plutons with crustal affinities (Tanque Granite, Pérez and Coira, 1998, a strike-slip component with left lateral motion is required to explain the NE–SW to E–W extension recorded by shallow–plunging stretching lineation (Fig. 2). This strike-slip component originates dilatation structures enhancing the basic magma ascent. The ascent and emplacement of these magmas took place contemporary with or close to contraction, although their genesis can be linked to extensional periods. Additionally, stretching parallel to the orogen might have occurred during the contractional periods, as is the case where intense thermal anomalies (Cruden et al., 2003) generate structures that allow plutons to be emplaced.

An extensional framework associated with a thermal anomaly and lithospheric thinning, including short contractional events and strike-slip components as in extensional as well as in shortening episodes, defines a complex picture.

Deformational, magmatic and metamorphic events like those observed in the Cobres and Tanque ranges provoke stratigraphic discontinuities in the contemporaneous basins such as those described in the Cordillera Oriental (Salfity et al., 1984; Moya, 1999; Astini, 2003).

After the late Arenigian, the magmatism drastically decreased, contractional deformation dominated, and the basin that received the Upper Ordovician deposits was generated (Upper Puna Turbidite Complex, Bahlburg, 1990). In this context, the zones occupied by the Western and Eastern Eruptive Belts could concentrate ductile deformation, creating uplifted regions that supplied deposits to the Upper Turbidite Complex.

In conclusion, the Ordovician tectono-magmatic evolution records two main stages. The first stage lasted from the Tremadocian to the early Arenigian dominated by extension. During that stage a bimodal magmatism took place represented by mesosilicic rocks with crustal affinities and initially, basic rocks with MORB-arc signature, succeeded at the Tremadocian–Arenigian boundary by one with OIB-type rocks. A later Arenigian stage lasted until the late Arenigian during which extensional and contractional conditions occurred diachronously along the basin, as was observed along the Tanque–Cochinoca–Escaya regions, the last with late basic OIB-like records associated to dacitic members.

The geochemical characteristics of the basic magmas erupted are attributed, considering the presented data, to a combination of factors such as variably depleted mantle sources, additions of continental crust and/or subduction components, and variations in the degree of melting in the source. These factors probably were controlled by episodical changes – both in time and space - in the extensional conditions which could affect the configuration of the basin. The variable chemistry of the basic rocks, the presence of siliceous magmatic rocks with crustal signatures and the contractional events record the evolution in the northeastern Puna of a back-arc, in which contractional episodes took place.

Acknowledgements

We are grateful to S. Ribeiro Guevara, P. Flores and P. Cachizumba for carrying out INAA and FRX analyses of major and trace elements, respectively. Constructive reviews from S. Poma, F. Lucassen are also gratefully acknowledged. We thank Suzanne Kay for final revision of English editing and helpful suggestions. This work was funded by ANPCyT (PICT 07-08724), SECTER-UNJU 08/E015 and CIUNSa (P. 1586 and 1235).

References

Astini, R., 2003. The Ordovician proto-Andean basins. In: Benedetto, J.L. (Ed.), Ordovician Fossils of Argentina, Secretaría de Ciencia y Tecnología. Universidad Nacional de Córdoba, pp. 1–74.

Bahlburg, H., 1990. The Ordovician Puna basin in the Puna of NW Argentina and N Chile: geodynamic evolution from back-arc to foreland basin. Geotektonische Forschungen 75, 1–107.

Bahlburg, H., Hervé, F., 1997. Geodynamic evolution and tectonostratigraphic terranes of northwestern Argentina and northern Chile. Geological Society of America Bulletin 109, 869–884.

Benedetto, J.L., Brussa, E.D., Pompei, J.F., 2002. El Ordovícico de la región de Susques–Huancar (Puna Oriental de Jujuy): precisiones sobre su edad y significado estratigráfico. 15° Congreso Geológico Argentino, El Calafate Actas 1, 572–577.

Bierlein, F.P., Stein, H.J., Coira, B., Reynolds, P., 2006. Timing of gold and crustal evolution of the Palaeozoic south central Andes, NW Argentina-implications for the endowment of orogenic belts. Earth and Planetary Science Letters 245, 702–721.

Blasco, G., Villar, L., Zappettini, E., 1996. Los complejos ofiolíticos desmembrados de la Puna Argentina, provincias de Salta y Catamarca. 13° Congreso Geológico Argentino y 3 Congreso Exploración de Hidrocarburos, Bs. Aires, Actas 3, 653–667.

Bock, B., Bahlburg, H., Wörner, G., Zimmermann, U., 2000. Tracing crustal evolution in the southern central Andes from Late Precambrian to Permian with geochemical and Nd and Pb isotope data. Journal of Geology 108, 515–535.

Breitkreuz, C., Bahlburg, H., Delakowitz, B., Pichowiak, S., 1989. Volcanic events in the Paleozoic central Andes. Journal of South American Earth Sciences 2, 171–189.

Cann, J.R., 1970. Rb, Sr ,Y, Zr and Nb in some ocean floor basaltic rocks. Earth Planetary Science Letters 10, 7–11.

Coira, B., Darren, J., 2002. Magmatismo ultrabásico–básico alcalino sin extensional arenigiano en el flanco sudoccidental de la Sierra de Aguilar, Prov. de Jujuy. 15° Congreso Geológico Argentino, El Calafate, Actas 2, 122–127.

Coira, B., Koukharsky, M., 2002. Ordovicician volcanic activity en the Puna, Argentina. In: Aceñolaza, F.G. (Ed.), Aspects of the Ordovician System in Argentina, Serie de Correlación Geológica, vol. 16. INSUGEO, Tucumán, pp. 267–280.

Coira, B., Koukharsky, M., 1991. Lavas en almohadillas ordovícicas en el Cordón Escaya, Puna Septentrional, Argentina. 6° Congreso Geológico Chileno, Actas I A-5, 674–678.

Coira, B., Kay, S.M., Pérez, B., Woll, B., Hanning, M., Flores, P., 1999. Magmatic sources and tectonic setting of Gondwana margin Ordovician magmas, northern Puna of Argentina and Chile. In: Ramos, V.A., Keppie, J.D., (Eds.), Laurentia–Gondwana Connections before Pangea. Geological Society of America Special Paper, vol. 336. pp. 145–170.

Coira, B., Koukarsky, M.L., Ribeiro Guevara, S., 2002. Magmatismo básico del Paleozoico Inferior en la Sierra de la Quebrada Honda, Puna Catamarqueña. Argentina. 15° Congreso Geológico Argentino, El Calafate, Actas, 115–121.

Coira, B., Caffe, P., Ramírez, A., Chayle, W., Díaz, A., Rosas, S., Pérez, A., Pérez, B., Orozco, O., Martínez, M., 2004. Descripción de la Hoja Geológica 2366–1 "Mina Pirquitas". Boletín del Servicio Geológico Minero Argentino 269, 1–123.

Coira, B., Díaz, A., Ramírez, A., Ribeiro Guevara, S., 2005. Volcanismo silíceo en la Quebrada de Taique, sus implicancias en la evolución de la Faja Magmática Oriental de la Puna, Argentina. 16° Congreso Geológico Argentino, La Plata, Actas I, 709–716.

Collins, W.J., 2002. Nature of extensional accretionary orogens. Tectonics 21(4), doi: 101029/2000TC001271.

Cruden, A., Nasseri, M.B., Pysklywec, R., 2003. Analogue versus numerical vise models of wide hot convergent orogens: influence of lateral flow on development of 3D strain fields and topography. Geophysical Research 5, 11476. Abstracts.

Fryer, P., Taylor, B., Langmuire, C.H., Hochstaedter, A.G., 1990. Petrology and geochemistry of lavas from the Sumisu and Torishima backarc rifts. Earth Planetary Science Letters 100, 161–178.

Haschke, M., Deeken, A., Insel, N., Grove, M., Smichtt, A., 2005. Growth pattern of the Andean Puna plateau constrained by apatite (U/Th)/He, K-feldspar $^{40}Ar/^{39}Ar$, and zircon U–Pb geochronology. In: Sixth International Symposium on Andean Geodynamics (ISAG 2005, Barcelona), Extended Abstracts. pp. 360–363.

Hawkins, T.R.W., 1970. Hornblende gabbros and picrites at Rhiw, Caernarvonshire. Geological Journal 7, 1–24.

Hawkins, J.W., 1995. Evolution of the Lau Basin–Insights from ODP Leg 135. American Geophysical Union Active margins and marginal basins of the Western Pacific. Geophysical Monograph 88, 125–173.

Hofmann, A.W., 1988. Chemical differentiation of the Earth in relationship between mantle continental crust and ocenic crust. Earth Planetary Science Letters 90, 297–314.

Hongn, F., 1994. Estructuras precámbricas y paleozoicas del basamento del borde oriental de la Puna; su aplicación para el análisis regional de la faja eruptiva. Revista de la Asociación Geológica Argentina 49 (3–4), 256–268.

Hongn, F., Mon, R., 1999. La deformación ordovícica en el borde oriental de la Puna. In: En Gonzalez Bonorino, G., Omarini, R., Viramonte, J.G., (Eds.), Geología del Noroeste Argentino. XIV Congreso Geológico Argentino, Salta, Relatorio, vol. 1. pp. 212–216.

Hongn, F., Mon, R., Acuña, P., Kirschbaum, A., Menegatti, N., 2006. Deformación intraordovícica en la sierra de Cobres. Asociación Geológica Argentina, Serie D 10, 186–192.

Kirschbaum, A., Menegatti, N., Hongn, F., Coira, B., Ribeiro Guevara, S., Brod, J.A., 2005. Magmatismo básico en la Sierra de Cobres, Puna Oriental, Salta. 16° Congreso Geológico Argentino, La Plata, Actas CD Trabajo 401, 3–4.

Kirschbaum, A., Hongn, F., Menegatti, N., 2006. The Cobres Plutonic Complex, eastern Puna (NW Argentina): petrological and structural constraints for Lower Paleozoic magmatism. Journal of South American Earth Sciences 21, 252–266.

Kleine, T., Mezger, K., Zimmermann, U., Münker, C., Bahlburg, H., 2004. Crustal evolution along the early ordovician proto-Andean margin of Gondwana: trace element and isotope evidence from the Complejo Igneo Pocitos (Northwestern Argentina). The Journal of Geology 112, 503–520.

Koukharsky, M., Coira, B., Morello, O., 1989. Volcanismo ordovícico de la Sierra de Guayaos, Puna salteña: características petrológicas e implicancias tectónicas. Asociación Geológica Argentina Revista 44, 207–216.

Koukharsky, M., Torres, C.R., Etcheverría, M., Vaccari, N.E., Waisfeld, B.G., 1996. Episodios volcánicos del Tremadociano y del Arenigiano en Vega Pinato, Puna salteña, Argentina. 13° Congreso Geológico Argentino y 3 Congreso de Exploración de Hidrocarburos, Actas 5, 535–542.

Koukharsky, M., Quenardelle, S., Litviak, V., Page, S., Maisonave, E.B., 2002. Plutonismo del Ordovícico inferior en el norte de la sierra de Macón, provincia de Salta. Revista de la Asociación Geológica Argentina 57 (2), 173–181.

Lork, A., Bahlburg, H., 1993. Precise U–Pb ages of monazites from the faja eruptiva de la Puna oriental, and the Cordillera Oriental, NW Argentina. 12° Congreso Geológico Argentino y 2 Congreso de Exploración de Hidrocarburos, Mendoza, Actas 4, 1–6.

Lucassen, F., Becchio, R., 2003. Timing of high-grade metamorphism: Early Paleozoic U–Pb formation ages of titanite indicate long-standing high-T conditions at the western margin of Gondwana (Argentina, 26–29°S). Journal of Metamorphic Geology 21, 649–662.

Lucassen, F., Becchio, R., Wilke, H.G., Thirlwall, M.F., Viramonte, J., Franz, G., Wemmer, K., 2000. Proterozoic-Paleozoic development of the basement of the Central Andes (18°–26°) – a mobile belt of the South American craton. Journal of South American Earth Sciences 13, 697–715.

Lucassen, F., Franz, G., Thirlwall, M., Mezger, K., 1999. Crustal recycling of metamorphic basement: late Paleozoic granitoids of Northern Chile (~22°S). Implications for the composition of the Andean crust. Journal of Petrology 40 (10), 1527–1551.

Lucassen, F., Becchio, R., Harmon, R., Kasemann, S., Franz, G., Trumbull, R., Wilke, H.G., Romer, R.L., Dulski, P., 2001. Composition and density model of the continental crust at an active continental margin –– the central Andes between 21° and 27°S. Tectonophysics 341 (2001), 195–223.

Martínez, M., Brussa, E.D., Pérez, B., Coira, B., 1999. Ordovícico de la Sierra de Quichagua (Puna nororiental argentina): litofacies volcanosedimentarias y graptofaunas. 14° Congreso Geológico Argentino, Actas 1, 347–350.

Méndez, V., Navarini, A., Plaza, D., Viera, O., 1973. Faja Eruptiva de la Puna Oriental. 5° Congreso Geológico Argentino, Actas 4, 147–158.

Moya, M.C., 1999. El Ordovícico de los Andes del Norte Argentino. In: González Bonorino, G., Omarini, R., Viramonte, J., (Eds.), Geología del Noroeste Argentino. 14° Congreso Geológico Argentino, Salta, Relatorio, vol. 1. pp. 134–152.

Niemeyer, H., 1989. El complejo ígneo-sedimentario del Cordón de Lila, región de Antofagasta. Significado tectónico. Revista Geológica de Chile 16, 163–181.

Palma, M.A., Parica, P., Ramos, V., 1986. El granito Archibarca: su edad y significado tectónico, provincia de Catamarca. Revista de la Asociación Geológica Argentina 41, 414–419.

Pearce, J.A., 1996. A user's guide to basalt discriminations diagrams. In: Wyman, D.A., (Ed.), Trace Element Geochemistry of Volcanic Rocks: Applications for Massive Sulphide Exploration. Geological Association of Canada. Short Courses Notes, vol. 12. pp. 79–113.

Pearce, J.A., Harris, N.B., Tindle, A.G., 1984. Trace element discrimination diagrams for the tectonic interpretation of granitic rocks. Journal of Petrology 25 (4), 956–983.

Pearce, J.A., Cann, J.R., 1973. Tectonic setting of basic volcanic rocks determined using trace element analysis. Earth Planetary Science Letters 19, 290–300.

Pearce, J.A., Norry, M.J., 1979. Petrogenetic implications of Ti, Zr, Y and Nb variations in volcanic rocks. Contributions to Mineralogy and Petrology 69, 33–47.

Pearce, J.A., Lippard, S.J., Roberts, S., 1984. Characteristics and tectonic significance of suprasucduction zone ophiolites. In: Marginal Basins Geology. Geological Society of America. Blackwell Scientific Publication, Oxford, pp. 77–93.

Pérez, B., Coira, B., 1998. El magmatismo ordovícico de la Sierra de Tanque, Puna septentrional, Argentina. 13° Congreso Geológico de Bolivia, Potosí, Memorias I, 229–235.

Salfity, J.A., Malanca, S., Brandán, M., Monaldi, R., Moya, C., 1984. La fase Guandacol en el norte de la Argentina. 9° Congreso Geológico Argentino, Bariloche, Actas 1, 555–567.

Saunders, A.D., Tarney, J., 1984. Geochemical characteristics of basaltic volcanism within back-arc basins. In: Kokelaar, B.P., Howells, M.F. (Eds.), Marginal Basin Geology, Geological Society. Blackwell Scientific Publications, Oxford, pp. 59–76.

Schwab, K., 1973. Die Stratigraphie in der Umgebung des Salar Cauchari (NW Argentinien). Ein Beitrag zur erdgeschichtlichen Entwicklung der Puna. Geotektonische Forschungen 43 (1), 168.

Vermeesch, P., 2006. Tectonic discrimination diagrams revisited. Geochemistry, Geophysics, and Geosystems, 7, Q06017, doi:10.1029/2005GC001092.

Winchester, J.A., Floyd, P.A., 1977. Geochemical discrimination of different magma series and their differentiation products using inmobile elements. Chemical Geology 20, 325–343.

Zimmermann, U., Bahlburg, H., 2003. Provenance analysis and tectonic setting of the Ordovician clastic deposits in the southern Puna basin, NW Argentina. Sedimentology 50, 1079–1104.